Momentum distributions, spin-dependent observables, and the D_2 parameter for ^{3}He breakup

A. P. Kobushkin*
Bogolyubov Institute for Theoretical Physics, Metrologicheskaya Street 14B, 03680 Kiev, Ukraine and National Technical University of Ukraine "KPI", Prospekt Peremogy 37, 03056 Kiev, Ukraine

E. A. Strokovsky†
Laboratory of High Energy Physics, Joint Institute for Nuclear Research, 141980, Dubna, Russia
(Dated:)

Using a recent parametrization of the fully antisymmetric three-nucleon wave function, based on the Paris and CD-Bonn potentials, we analyze the momentum distributions of constituents in ^{3}He, as well as the spin-dependent observables for $(^3\mathrm{He}, d)$ and $(^3\mathrm{He}, p)$ breakup reactions. Special attention is paid to the region of small relative momenta of the ^{3}He constituents, where a single parameter, D_2, has a determining role for the spin-dependent observables in the $d+p$ channel. This fact results in some useful relations between experimental observables.

PACS numbers: 25.30.Bf,13.40.-f,13.60.-Hb,13.88.+e

I. INTRODUCTION

Momentum distributions of one and two nucleon fragments in ^{3}He give important information about nuclear systems more complicated than the deuteron. They cast light on such interesting problems as the nucleon-nucleon interaction at short distances, the role of three-body interactions (the $3N$-forces), and non-nucleonic degrees of freedom in nuclei.

Precise data are currently available on the momentum distributions of the proton and the deuteron obtained with electromagnetic [1–4] and hadronic probes [5–7]. Data on the energy dependence of the differential cross sections of backward elastic ^{3}He(p,^{3}He)p scattering, which are related to the same momentum distributions, also exist [8, 9]. Furthermore, the spin-correlation parameter C_{yy} for this reaction was recently measured for first time [9]. Finally, the tensor polarization of the deuteron (sometimes called its "alignment") in the ^{12}C(^{3}He, d) reaction was also measured [10, 11]. Both this and the C_{yy} data [9] are sensitive to the spin structure of ^{3}He.

For a long time the lack of useful parametrizations of the three-nucleon wave function has made the theoretical analysis of these data difficult. However, a convenient parametrization of the fully antisymmetric three-nucleon wave function based on the Paris [12] and CD-Bonn [13] potentials has recently been presented [14], which we use here to calculate the momentum distributions in ^{3}He, as well as the spin-dependent observables, within the framework of the spectator model for the ^{3}He breakup reactions. Special attention is paid to the study of the two-body $^3\mathrm{He} \to d+p$ channel. We compare our results with other theoretical works and with existing experimental data.

In our analysis of spin-dependent observables for $(^3\mathrm{He}, d)$ and $(^3\mathrm{He}, p)$ reactions, we carefully consider their behavior in the region of small (below $\sim$ 150 MeV/c) internal momenta of the ^{3}He fragments, where a single quantity, known in the literature as the D_2 parameter, completely determines both the sign and the momentum dependence of the observables. Several relations between experimental observables in this region were obtained from this consideration. These provide useful checks on the consistency of the experimental database of spin-dependent observables because at low relative momenta of the ^{3}He fragments the model used for the breakup reactions works reasonably well.

The paper is organized as follows. In Sec. II we discuss the parametrization of the three-nucleon wave function used in the later work. Distributions of one- and two-nucleon constituents in ^{3}He are evaluated and compared with the results of other calculations in Sec. III. Various spin-dependent observables for $(^3\mathrm{He}, d)$ and $(^3\mathrm{He}, p)$ breakup are considered and discussed in Sec. IV. In Sec. V we compare our results with experiment within the "minimal relativization scheme" and discuss briefly the limitations of our approach. Conclusions and discussion are presented in Sec. VI.

II. THE PARAMETRIZATION OF THE THREE-NUCLEON WAVE FUNCTION

We here give a review of the parametrization of the ^{3}He wave function [14]. Working in the framework of the so-called channel spin coupling scheme (Ref. [15]), the authors of Ref. [14] restricted themselves to five partial waves,

$$\left|\left[\left((\ell s) j \tfrac{1}{2}\right) KL\right] \tfrac{1}{2}\right\rangle, \qquad (1)$$

where ℓ, j, and s are the orbital, total, and spin angular momenta for the pair (the 2$^{\mathrm{nd}}$ and 3$^{\mathrm{rd}}$ nucleons), and L

*Electronic address: kobushkin@bitp.kiev.ua
†Electronic address: Eugene.Strokovsky@sunse.jinr.ru

TABLE I: Quantum numbers of the ^{3}He partial waves. Here s, τ, ℓ and j are spin, isospin, orbital and total angular momenta of the pair; L and K are relative angular momenta for the spectator and the channel spin, respectively.

Channel No	Label	ℓ	s	j^π	K	L	τ
1	^1s_0S	0	0	0^+	1/2	0	1
2	^3s_1S	0	1	1^+	1/2	0	0
3	^3s_1D	0	1	1^+	3/2	2	0
4	^3d_1S	2	1	1^+	1/2	0	0
5	^3d_1D	2	1	1^+	3/2	2	0

and K are the relative orbital angular momentum for the spectator (the 1$^{\rm st}$ nucleon) and the channel spin, respectively. Coulomb effects are not included. The appropriate quantum numbers of the partial waves are collected in Table I.

We use the standard definition of the Jacobi coordinates $\mathbf{r}$ and $\boldsymbol{\rho}$ in the three-particle system and the corresponding momenta $\mathbf{p}$ and $\mathbf{q}$:

$$\begin{aligned} \mathbf{r}_1 &= \mathbf{R} + \tfrac{2}{3}\boldsymbol{\rho}, & \mathbf{p}_1 &= \tfrac{1}{3}\mathbf{P} + \mathbf{q}\,, \\ \mathbf{r}_2 &= \mathbf{R} - \tfrac{1}{3}\boldsymbol{\rho} + \tfrac{1}{2}\mathbf{r}, & \mathbf{p}_2 &= \tfrac{1}{3}\mathbf{P} - \tfrac{1}{2}\mathbf{q} + \mathbf{p}\,, \\ \mathbf{r}_3 &= \mathbf{R} - \tfrac{1}{3}\boldsymbol{\rho} - \tfrac{1}{2}\mathbf{r}, & \mathbf{p}_3 &= \tfrac{1}{3}\mathbf{P} - \tfrac{1}{2}\mathbf{q} - \mathbf{p}\,. \end{aligned} \tag{2}$$

Here $\mathbf{R}$ is the coordinate of the nucleus center of mass (with $\mathbf{P}$ being the total momentum of the nucleus), $\boldsymbol{\rho}$ is the radius vector from the center of mass of the nucleon pair to the nucleon 1 (the corresponding momentum is $\mathbf{q}$), and $\mathbf{r}$ is the separation between the nucleons in the pair (the corresponding momentum is $\mathbf{p}$).

Explicitly, the wave function of ^{3}He in momentum space reads

$$\begin{aligned} \Psi_\sigma(\mathbf{p},\mathbf{q}) = \sum_\xi \Bigg\{ & \frac{1}{4\pi}\delta_{\xi\sigma} \sum_{\tau_3,t_3} \left\langle 1\tfrac{1}{2}\tau_3 t_3 \mid \tfrac{1}{2}\tfrac{1}{2}\right\rangle \psi_1(p,q)\,|00;1\tau_3\rangle\,\chi_{\xi t_3} + \sum_{s_3}\Bigg[\frac{1}{4\pi}\left\langle 1\tfrac{1}{2}s_3\xi \mid \tfrac{1}{2}\sigma\right\rangle \psi_2(p,q) \\ & -\sqrt{\frac{1}{4\pi}}\sum_{L_3K_3} \left\langle 1\tfrac{1}{2}s_3\xi \mid \tfrac{3}{2}K_3\right\rangle \left\langle \tfrac{3}{2}2K_3L_3 \mid \tfrac{1}{2}\sigma\right\rangle Y_{2L_3}(\widehat{\mathbf{q}})\psi_3(p,q) \\ & -\sqrt{\frac{1}{4\pi}}\sum_{\ell_3 M} \langle 12s_3\ell_3|1M\rangle \left\langle 1\tfrac{1}{2}M\xi \mid \tfrac{1}{2}\sigma\right\rangle Y_{2\ell_3}(\widehat{\mathbf{p}})\psi_4(p,q) \\ & +\sum_{\ell_3 M L_3 K_3} \langle 12s_3\ell_3|1M\rangle \left\langle 1\tfrac{1}{2}M\xi \mid \tfrac{3}{2}K_3\right\rangle \left\langle \tfrac{3}{2}2K_3L_3 \mid \tfrac{1}{2}\sigma\right\rangle Y_{2L_3}(\widehat{\mathbf{q}})Y_{2\ell_3}(\widehat{\mathbf{p}})\psi_5(p,q)\Bigg]\,|1s_3;00\rangle\,\chi_{\xi\frac{1}{2}}\Bigg\}\,, \end{aligned} \tag{3}$$

where σ and ξ are the spin projections of ^{3}He and the spectator nucleon, t_3 is the isospin projection of the spectator nucleon, M is the projection of the total angular momentum of the pair, and $\chi_{\xi t_3}$ and $|ss_3;\tau\tau_3\rangle$ are the spin-isospin wave functions of the spectator nucleon and the pair, respectively.

Note, that in Eq. (3) we use the following convention for angular momentum summation

$$j + \tfrac{1}{2} \to K, \qquad K + L \to \tfrac{1}{2}. \tag{4}$$

Other conventions are often used in the literature, for example:

$$j + \tfrac{1}{2} \to K, \qquad L + K \to \tfrac{1}{2} \tag{5}$$

and

$$\tfrac{1}{2} + j \to K, \qquad L + K \to \tfrac{1}{2}. \tag{6}$$

The convention of Eq. (5) was used, in particular, in Ref. [16], whereas that of Eq. (6) was exploited in Ref. [17].

Due to the properties of the Clebsch-Gordan coefficients under permutations, for example $\left\langle \frac{3}{2}\,2\,K_3\,L_3|\frac{1}{2}\xi\right\rangle = -\left\langle 2\,\frac{3}{2}\,L_3\,K_3|\frac{1}{2}\xi\right\rangle$, some of the wave function components have opposite signs in different conventions. For example, using Eq. (5) rather than Eq. (4) would result in $\psi_3(p,q) \to -\psi_3(p,q)$ and $\psi_5(p,q) \to -\psi_5(p,q)$. Similarly, the use of Eq. (6) instead of Eq. (4) would give $\psi_2(p,q) \to -\psi_2(p,q)$, $\psi_3(p,q) \to -\psi_3(p,q)$, $\psi_4(p,q) \to -\psi_4(p,q)$, and $\psi_5(p,q) \to -\psi_5(p,q)$, while $\psi_1(p,q)$ would not change sign.

The partial waves are approximated by the following functions of the two momenta p and q:

$$\psi_\nu(p,q) = v_1^\nu(p)w_1^\nu(q) + v_2^\nu(p)w_2^\nu(q), \tag{7}$$

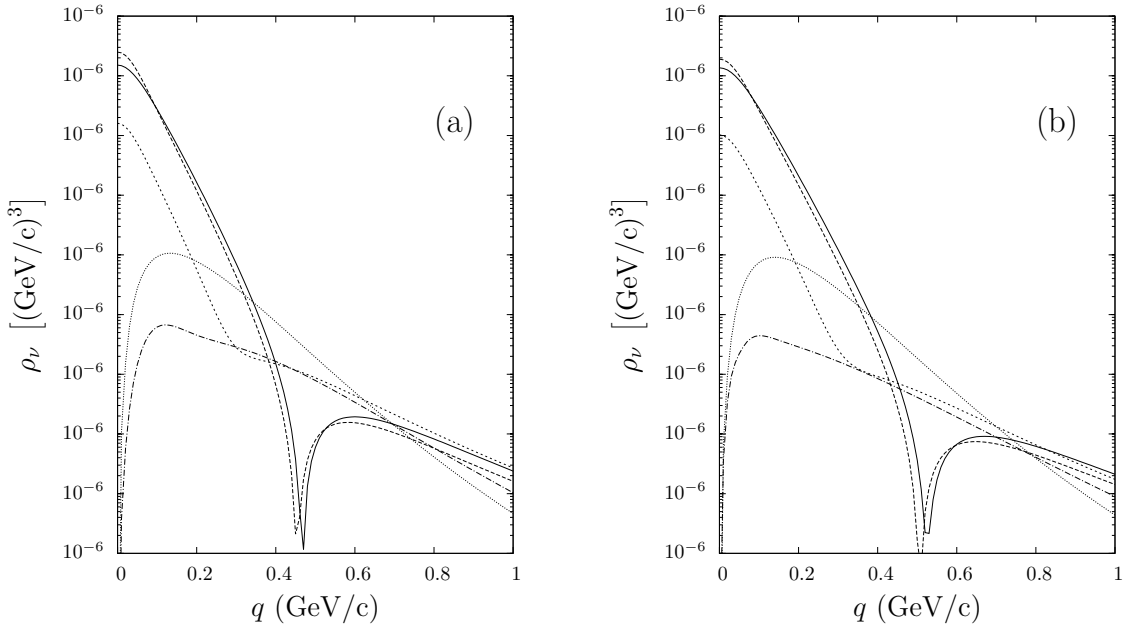

FIG. 1: One-nucleon momentum distributions in partial channels for the Paris [12] (a) and CD-Bonn [13] (b) potentials. Long-dashed lines, ^1s_0S; solid lines, ^3s_1S; short-dashed lines, ^3d_1S; dotted lines, ^3s_1D; and dash-dotted lines, ^3d_1D.

where

$$v_i^\nu(p) = \sum_{n=1}^{5} \frac{a_{n,i}^\nu}{p^2 + (m_{n,i}^\nu)^2}, \qquad w_i^\nu(q) = \sum_{n=1}^{5} \frac{b_{n,i}^\nu}{q^2 + (M_{n,i}^\nu)^2}. \tag{8}$$

The parameters are restricted by the usual constraints for S and D waves:

$$\sum_{n=1}^{5} a_{n,i}^\nu = \sum_{n=1}^{5} b_{n,i}^\nu = 0. \tag{9}$$

There are additional constraints for D waves:

$$\sum_{n=1}^{5} a_{n,i}^\nu (m_{n,i}^\nu)^2 = \sum_{n=1}^{5} b_{n,i}^\nu (M_{n,i}^\nu)^2 = 0, \qquad \sum_{n=1}^{5} \frac{a_{n,i}^\nu}{(m_{n,i}^\nu)^2} = \sum_{n=1}^{5} \frac{b_{n,i}^\nu}{(M_{n,i}^\nu)^2} = 0. \tag{10}$$

The full ^{3}He wave function is normalized by the condition

$$\sum_{\nu=1}^{5} \int_0^\infty dq \int_0^\infty dp\, q^2 p^2 \left|\psi_\nu(p,q)\right|^2 = 1. \tag{11}$$

III. MOMENTUM DISTRIBUTIONS

A. One-nucleon distributions

Assuming final plane waves, the one-nucleon momentum distribution in a partial channel ν becomes

$$\rho_\nu(q) = \frac{3}{4\pi} \int_0^\infty dp\, p^2 \left|\psi_\nu(p,q)\right|^2, \tag{12}$$

where the coefficient of 3 is the square of a spectroscopic factor. The distributions for each partial channel are displayed in Fig. 1. It is important to note that the distributions for the ^1s_0S and ^3s_1S channels are very similar in both their magnitude and their momentum dependence.

The values of the partial channel probabilities, defined as

$$P_\nu = \frac{1}{3} \int d^3q\, \rho_\nu(q) = \int dp\, dq\, p^2 q^2 |\psi_\nu(p,q)|^2, \tag{13}$$

are given in Table II.

The momentum distribution of a nucleon N with spin and isospin projections ξ and t_3 in the ^{3}He with spin projection σ is

$$N_{\sigma(\xi t_3)}(\mathbf{q}) = 3 \sum_{s s_3 \tau \tau_3} \int d^3p \left| \chi^\dagger_{\xi t_3} \langle s s_3 \tau \tau_3 | \, \Psi_\sigma(\mathbf{p},\mathbf{q}) \right|^2. \tag{14}$$

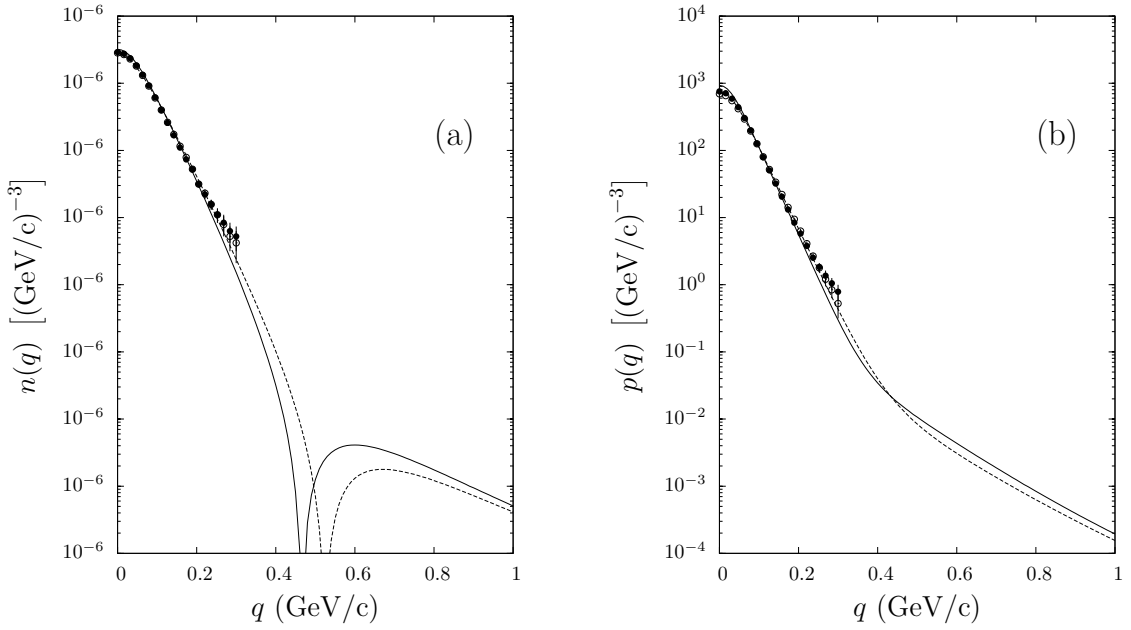

FIG. 2: The neutron (a) and proton (b) momentum distributions. The solid and dashed curves are for the Paris and CD-Bonn potentials, respectively. The solid and open circles represent results of variational calculations [18] obtained using the Urbana and Argonne potentials, respectively.

In the neutron case, Eq. (14) reduces to [1]

$$\begin{aligned} n_{\sigma\xi}(q) &= \delta_{\sigma\xi}\frac{1}{2\pi}\int_0^\infty \left[\psi_1(p,q)\right]^2 p^2 dp \\ &= \tfrac{2}{3}\delta_{\sigma\xi}\rho_1(q) \equiv \delta_{\sigma\xi} n(q). \end{aligned} \tag{15}$$

Note that the number of neutrons $\mathcal{N}_n$ in ^{3}He is given by the integral $\mathcal{N}_n = \int d^3q\, n(q) = 1$ and that the ψ_1 component must be normalized as

$$\int dp\, dq\, p^2 q^2 \left[\psi_1(p,q)\right]^2 = \tfrac{1}{2}\ . \tag{16}$$

Here and below we use $p_{\sigma\xi}$ and $n_{\sigma\xi}$ instead of $N_{\sigma(\xi,\frac{1}{2})}$ and $N_{\sigma(\xi,-\frac{1}{2})}$, respectively.

The resulting neutron momentum distributions, $n(q)$, for the Paris and CD-Bonn potentials are shown in Fig. 2(a). We also compare the results with variational calculations [18] based on the Argonne and Urbana potentials.

Using the results given in Appendix A, we get the followinf for the momentum distribution of protons with spin projection $\frac{1}{2}$ and $-\frac{1}{2}$ in the ^{3}He having spin projection $+\frac{1}{2}$:

$$\begin{aligned} p_{\frac{1}{2}\frac{1}{2}}(q,\theta) &= \frac{1}{3}\left[\rho_1(q)+\rho_2(q)+\rho_4(q)\right] \\ &+ \frac{1}{2}\left(\cos^2\theta + \frac{1}{3}\right)\left[\rho_3(q)+\rho_5(q)\right] \\ &+ \sqrt{2}\left(\frac{1}{3} - \cos^2\theta\right)\left[\rho_{23}(q)+\rho_{45}(q)\right], \\ p_{\frac{1}{2}-\frac{1}{2}}(q,\theta) &= \frac{2}{3}\left[\rho_2(q)+\rho_4(q)\right] \\ &+ \frac{1}{2}\left(-\cos^2\theta + \frac{5}{3}\right)\left[\rho_3(q)+\rho_5(q)\right] \\ &- \sqrt{2}\left(\frac{1}{3} - \cos^2\theta\right)\left[\rho_{23}(q)+\rho_{45}(q)\right], \end{aligned} \tag{17}$$

where θ is the angle between the z axis (the quantization axis) and the proton momentum $\mathbf{q}$. The function $\rho_{\mu\nu}(q)$ is defined as

$$\rho_{\mu\nu}(q) = \frac{3}{4\pi}\int_0^\infty dp\, p^2 \psi_\mu(p,q)\psi_\nu(p,q), \qquad \mu \neq \nu. \tag{18}$$

(When $\mu = \nu$ it is sufficient to retain a single index.)

The momentum distribution of the proton, given by the sum of $p_{\frac{1}{2}\frac{1}{2}}(q,\theta)$ and $p_{\frac{1}{2}-\frac{1}{2}}(q,\theta)$, does not depend upon the angle θ:

$$\begin{aligned} p(q) =& p_{\frac{1}{2}\frac{1}{2}}(q,\theta) + p_{\frac{1}{2}-\frac{1}{2}}(q,\theta) = \frac{1}{3}\rho_1(q) + \rho_2(q) \\ &+ \rho_3(q) + \rho_4(q) + \rho_5(q). \end{aligned} \tag{19}$$

Figure 2(b) displays the proton momentum distribution calculated using four potentials.

[1] It must be noted that normalizations of the proton (N_p) and neutron (N_n) momentum distributions in Table 7 of Ref. [18] differ from those used here; they can be compared with our $n(q)$ and $p(q)$ after multiplication by a renormalization factor of $(2\pi)^{-3}$.

TABLE II: The partial channel probabilities P_ν in ^{3}He.

	^1s_0S	^3s_1S	^3s_1D	^3d_1S	^3d_1D
Paris	0.5000	0.4600	0.0282	0.0103	0.0015
CD-Bonn	0.5000	0.4658	0.0231	0.0102	0.0009

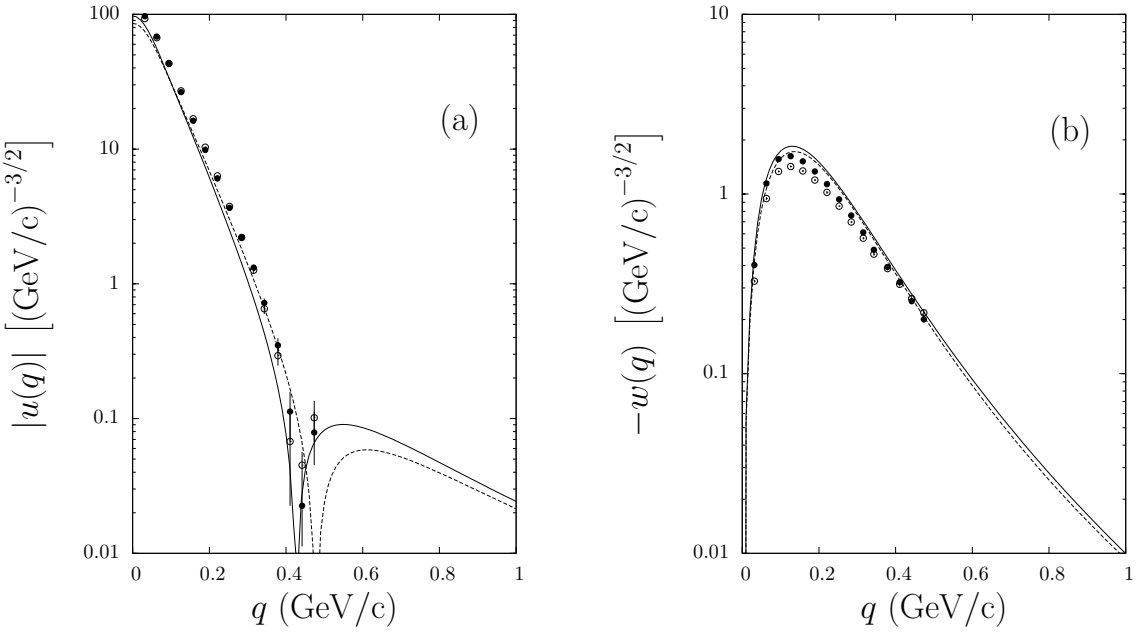

FIG. 3: The $u(q)$ (a) and $w(q)$ (b) wave functions of the relative deuteron-proton motion in ^{3}He. The notations are the same as those in Fig. 2.

¿From Eqs. (16), (17), and (19) and the normalization condition of Eq. (11), it follows immediately that the number of protons in ^{3}He is $\mathcal{N}_p = \int d^3q\, p(q) = 2$.

B. Two-nucleon momentum distributions

We define the two-body amplitudes $A_{dp}(M,\xi,\sigma,\mathbf{q})$ as

$$\begin{aligned} &A_{dp}(M,\xi,\sigma,\mathbf{q}) \\ &= \sqrt{3}\int d^3r\, d^3\rho\, \Psi_d^\dagger(M,\mathbf{r})\chi^\dagger_{\xi\frac{1}{2}} \exp\left(-i\boldsymbol{\rho}\cdot\mathbf{q}\right)\Psi_\sigma(\mathbf{r},\boldsymbol{\rho}) \\ &= (2\pi)^{\frac{3}{2}}\sqrt{3}\int d^3p\, {\psi_d}^\dagger(M,\mathbf{p})\chi^\dagger_{\xi\frac{1}{2}}\Psi_\sigma(\mathbf{p},\mathbf{q}) \\ &= (2\pi)^{\frac{3}{2}}\left\{\sqrt{\frac{1}{4\pi}}\langle 1\tfrac{1}{2}M\xi|\tfrac{1}{2}\sigma\rangle u(q)\right. \\ &\left. - \sum_{K_3L_3}\langle 1\tfrac{1}{2}M\xi|\tfrac{3}{2}K_3\rangle\langle 2\tfrac{3}{2}L_3K_3|\tfrac{1}{2}\sigma\rangle Y_{2L_3}(\widehat{q})w(q)\right\}, \end{aligned} \tag{20}$$

where $\sqrt{3}$ is the spectroscopic factor, $\Psi_d(M,\mathbf{r})$ and $\psi_d(M,\mathbf{p})$ are the deuteron wave function in coordinate and momentum space, respectively, M and ξ are spin projections of the deuteron and the proton and

$$\begin{aligned} u(q) &= \sqrt{3}\int_0^\infty dp\, p^2\left[u_d(p)\psi_2(p,q) + w_d(p)\psi_4(p,q)\right], \\ w(q) &= -\sqrt{3}\int_0^\infty dp\, p^2\left[u_d(p)\psi_3(p,q) + w_d(p)\psi_5(p,q)\right], \end{aligned} \tag{21}$$

where $u_d(p)$ and $w_d(p)$ are the deuteron S and D wave functions, respectively. [2]

Equation (20) allows us to relate the amplitudes $A^{00}_{dp}(1,-\frac{1}{2},\frac{1}{2},q)$ and $A^{22}_{dp}(1,-\frac{1}{2},\frac{1}{2},q)$ of Schiavilla *et*

[2] For the convention given by Eq. (5) one must replace $w(q)$ by $-w(q)$. This notation was used, e.g., in Ref. [19].

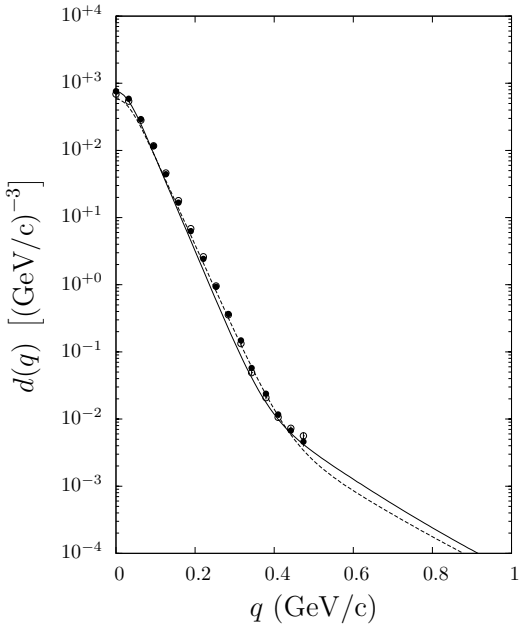

FIG. 4: The momentum distribution of the deuterons in ^{3}He. The notations are the same as those in Fig. 2.

al. [18] to the wave functions $u(q)$ and $w(q)$:

$$\begin{aligned} u(q) &= \left(\frac{1}{2\pi}\right)^{\frac{3}{2}} \frac{A^{00}_{dp}(1,-\frac{1}{2},\frac{1}{2},q)}{\langle 1\frac{1}{2}1-\frac{1}{2}|\frac{1}{2}\frac{1}{2}\rangle} \\ &= \left(\frac{1}{2\pi}\right)^{\frac{3}{2}} \sqrt{\frac{3}{2}} A^{00}_{dp}(1,-\frac{1}{2},\frac{1}{2},q), \\ w(q) &= \left(\frac{1}{2\pi}\right)^{\frac{3}{2}} \frac{A^{22}_{dp}(-1,-\frac{1}{2},\frac{1}{2},q)}{\langle 1\frac{1}{2}-1-\frac{1}{2}|\frac{3}{2}-\frac{3}{2}\rangle\langle\frac{3}{2}2-\frac{3}{2}2|\frac{1}{2}\frac{1}{2}\rangle} \\ &= \left(\frac{1}{2\pi}\right)^{\frac{3}{2}} \sqrt{\frac{5}{2}} A^{22}_{dp}(-1,-\frac{1}{2},\frac{1}{2},q). \end{aligned} \tag{22}$$

The $u(q)$ and $w(q)$ wave functions calculated from different potentials are displayed in Fig. 3 and the momentum distribution of the deuterons

$$d(q) = u^2(q) + w^2(q). \tag{23}$$

is shown in Fig. 4.

The effective numbers of the deuterons in ^{3}He, $\mathcal{N}_d = \int d^3q\, q^2 d(q)$, are 1.39 and 1.36 for the Paris and CD-Bonn potentials, respectively. These can be compared with $\mathcal{N}_d = 1.38$ obtained in variational calculations [18] with both the Argonne and Urbana potentials. The probabilities of the D-wave in the $d+p$ configuration, $P_D = \int dq\, q^2 w^2(q)/[\int dq\, q^2(u^2(q)+w^2(q))]$, are 1.53% and 1.43% for the Paris and CD-Bonn potentials, respectively.

IV. SPIN-DEPENDENT OBSERVABLES

A. Tensor analyzing powers and the D_2 parameter

In a plane wave Born approximation the tensor analyzing powers T_{20}, T_{21} and T_{22} of the (d,t) and $(d,^3\mathrm{He})$ reactions at low energies are determined by a single parameter D_2 used, for example, in Refs. [16, 20–22]:

$$D_2 = \frac{1}{15}\frac{\int_0^\infty dr\, r^4\, U(r)}{\int_0^\infty dr\, r^2\, W(r)} = \lim_{q\to 0}\frac{w(q)}{q^2 u(q)}, \tag{24}$$

i.e., $w(q)/u(q) \approx q^2 D_2$ at small q. In Eq. (24), $U(r)$ and $W(r)$ are the S and D waves of the $d+p$ component of the ^{3}He wave function in configuration space. The D_2 parameter is closely related to the asymptotic D to S ratio for the $p+d$ partition of the ^{3}He wave function, as is noted in Ref. [22].

The spin-dependent observables considered here depend upon the bilinear forms of S and D waves of the ^{3}He wave function and the behavior of their ratio at small q is completely governed by the D_2 parameter. In Table III we compare this parameter, calculated for the wave functions based on different potentials, with the values derived from experiment.

B. Tensor polarization of the deuteron

We start by considering the tensor polarization of the deuteron in (^{3}He,d) breakup, which is defined as

$$\rho_{20} = \frac{1}{\sqrt{2}}\frac{d\sigma_+ + d\sigma_- - 2d\sigma_0}{d\sigma_+ + d\sigma_- + d\sigma_0}\,, \tag{25}$$

where $d\sigma_+$, $d\sigma_-$, and $d\sigma_0$ are the breakup differential cross section for the deuteron with spin projections $+1$, -1, and 0 onto the quantization axis, which we take to be along the deuteron momentum, i.e., $\mathbf{q} = (0,0,-q)$. In the spectator model the differential cross sections of ^{3}He fragmentation in the deuteron with magnetic number M is proportional to

$$d\sigma(M) \propto \sum_{\xi,\sigma} |A_{dp}(M,\xi,\sigma,\vec{q})|^2\,, \tag{26}$$

times a coefficient that is independent of M.

With this quantization axis, $Y_{2L_3}(\hat{q}) \sim \delta_{L_3 0}$, and the cross sections are proportional to

$$\begin{aligned} d\sigma_+ = d\sigma_- &\propto \frac{1}{2}\left|A_{dp}(1,-\tfrac{1}{2},\tfrac{1}{2})\right|^2 \\ &\propto u^2(q) + \frac{1}{2}w^2(q) - \sqrt{2}u(q)w(q), \\ d\sigma_0 &\propto \frac{1}{2}\left(\left|A_{dp}(0,\tfrac{1}{2},\tfrac{1}{2})\right|^2 + \left|A_{dp}(0,-\tfrac{1}{2},-\tfrac{1}{2})\right|^2\right) \\ &\propto u^2(q) + 2w^2(q) + 2\sqrt{2}u(q)w(q) \end{aligned} \tag{27}$$

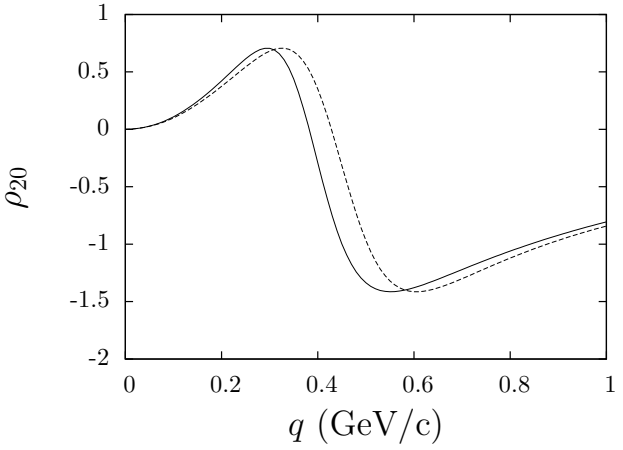

FIG. 5: Deuteron alignment calculated with ^{3}He wave functions for the Paris (solid) and CD-Bonn (dashed) potentials.

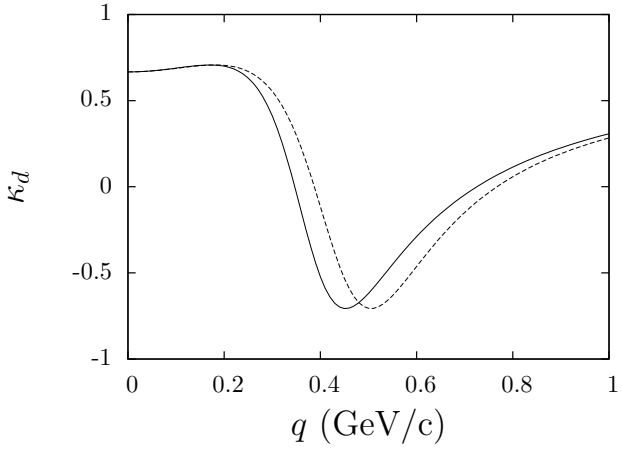

FIG. 6: Polarization transfer κ_d from ^{3}He to d for the Paris (solid) and CD-Bonn (dashed) potentials.

and

$$\rho_{20} = -\frac{1}{\sqrt{2}} \frac{2\sqrt{2}u(q)w(q) + w^2(q)}{u^2(q) + w^2(q)}. \tag{28}$$

It is clear from Eq. (28) that, even in the case of the breakup of an unpolarized ^{3}He, the deuteron spectator emitted at 0° has a tensor polarization. Note that at small q this results in $\rho_{20} \approx -2w(q)/u(q) = -2q^2 D_2$. The predictions for ρ_{20} obtained with the wave functions from the Paris and CD-Bonn potentials are shown in Fig. 5.

C. Polarization transfer from ^{3}He to d

We consider here the case when the quantization axes for the ^{3}He and the deuteron are parallel and both are perpendicular to the deuteron momentum. We define the coefficient of the vector-to-vector polarization transfer from polarized ^{3}He to deuteron (whose vector polarization is under consideration) as

$$\kappa_d = \sum_\xi \left[d\sigma(1,\xi,\tfrac{1}{2}) + d\sigma(-1,\xi,-\tfrac{1}{2}) - d\sigma(1,\xi,-\tfrac{1}{2}) - d\sigma(-1,\xi,\tfrac{1}{2}) \right] / \sum_{M,\xi,\sigma} d\sigma(M,\xi,\sigma), \tag{29}$$

where $d\sigma(M,\xi,\sigma) \propto |A_{dp}(M,\xi,\sigma,\vec{q})|^2$.

¿From invariance under space inversion we have

$$\begin{aligned} \sum_\xi d\sigma(1,\xi,\tfrac{1}{2}) &= \sum_\xi d\sigma(-1,\xi,-\tfrac{1}{2}), \\ \sum_\xi d\sigma(-1,\xi,\tfrac{1}{2}) &= \sum_\xi d\sigma(1,\xi,-\tfrac{1}{2}), \\ \sum_\xi d\sigma(0,\xi,\tfrac{1}{2}) &= \sum_\xi d\sigma(0,\xi,-\tfrac{1}{2}) \end{aligned} \tag{30}$$

and Eq. (29) reduces to

$$\kappa_d = \frac{\sum_\xi \left[d\sigma(1,\xi,\tfrac{1}{2}) - d\sigma(1,\xi,-\tfrac{1}{2}) \right]}{\sum_{M,\xi,\sigma} d\sigma(M,\xi,\tfrac{1}{2})}. \tag{31}$$

It is straightforward to show that

$$\begin{aligned} &d\sigma(1,\tfrac{1}{2},\tfrac{1}{2}) = d\sigma(-1,\tfrac{1}{2},\tfrac{1}{2}) = d\sigma(0,-\tfrac{1}{2},\tfrac{1}{2}) = 0, \\ &d\sigma(1,-\tfrac{1}{2},\tfrac{1}{2}) \propto \left(-\sqrt{\tfrac{2}{3}}u + \frac{1}{2}\sqrt{\tfrac{1}{3}}w \right)^2, \\ &d\sigma(-1,-\tfrac{1}{2},\tfrac{1}{2}) \propto \tfrac{3}{4}w^2, \\ &d\sigma(0,\tfrac{1}{2},\tfrac{1}{2}) \propto \left(-\sqrt{\tfrac{1}{3}}u + \tfrac{1}{2}\sqrt{\tfrac{2}{3}}w \right)^2 \end{aligned} \tag{32}$$

and the polarization transfer coefficient becomes

$$\kappa_d = \frac{2}{3} \left(\frac{u^2 - w^2 - uw/\sqrt{2}}{u^2 + w^2} \right). \tag{33}$$

We point out here that the expression given in Eq. (33) differs from in Eq. (5) of Ref. [23] by a factor 2. This factor was erroneously lost in that paper.

Results of calculations with ^{3}He wave functions from the Paris and CD-Bonn potentials are shown in Fig. 6.

The observables κ_d and ρ_{20} are related by:

$$\left(\frac{3}{2}\kappa_d \right)^2 + \left(\rho_{20} + \frac{1}{2\sqrt{2}} \right)^2 = \frac{9}{8}. \tag{34}$$

Furthermore, at small q

$$\kappa_d \approx \frac{2}{3} \left(1 - \frac{q^2 D_2}{\sqrt{2}} \right) \approx \frac{2}{3} \left(1 + \frac{\rho_{20}}{2\sqrt{2}} \right), \tag{35}$$

so that $\kappa_d \to 2/3$ when $q \to 0$.

TABLE III: $D_2(3N)$ parameter (in fm^2).

Paris	CD-Bonn	AV18 [18]	Urbana [18]	Experiment [22]
-0.2387	-0.2487	-0.27	-0.23	-0.259 ± 0.014

D. Polarization transfer from ^{3}He to p

The polarization transfer from ^{3}He to p is defined by:

$$\kappa_p = \frac{p_{\frac{1}{2}\frac{1}{2}} - p_{\frac{1}{2}-\frac{1}{2}}}{p_{\frac{1}{2}\frac{1}{2}} + p_{\frac{1}{2}-\frac{1}{2}}}, \tag{36}$$

where the $p_{\sigma\xi}$ are given by Eq. (17). At $\theta = 90^\circ$ this reduces to

$$\kappa_p = \frac{\rho_1 - \rho_2 - \rho_4 - 2(\rho_3 + \rho_5) + 2\sqrt{2}(\rho_{13} + \rho_{45})}{\rho_1 + 3(\rho_2 + \rho_3 + \rho_4 + \rho_5)}. \tag{37}$$

For the $d + p$ projection of the ^{3}He wave function, the proton momentum distributions are

$$\begin{aligned} \widetilde{p}_{\frac{1}{2}\frac{1}{2}}(q, 90^\circ) &= \frac{2\pi^2}{3}\left[u^2(q) - \sqrt{2}u(q)w(q) + \tfrac{1}{2}w^2(q)\right], \\ \widetilde{p}_{\frac{1}{2}-\frac{1}{2}}(q, 90^\circ) &= \frac{2\pi^2}{3}\left[2u^2(q) + \sqrt{2}u(q)w(q) + \tfrac{5}{2}w^2(q)\right] \end{aligned} \tag{38}$$

and hence

$$\widetilde{\kappa}_p = -\frac{u^2 + 2\sqrt{2}uw + 2w^2}{3(u^2 + w^2)}. \tag{39}$$

The behavior of κ_p and $\widetilde{\kappa}_p$ is shown in Fig. 7.

It is easy to see that the observables $\widetilde{\kappa}_p$ and ρ_{20} must be related because the spin-dependent observables under consideration are determined by the ratio of the two functions $u(q)$ and $w(q)$. One then finds

$$\widetilde{\kappa}_p = -\frac{1}{3}\left(1 - \sqrt{2}\rho_{20}\right), \tag{40}$$

so that at small q

$$\widetilde{\kappa}_p \approx -\frac{1}{3}\left(1 - 2\sqrt{2}q^2 D_2\right) \tag{41}$$

and hence $\widetilde{\kappa}_p \to -1/3$ when $q \to 0$.

A linear combination of the two polarization transfer coefficients has the following behavior at small q:

$$1 - (\widetilde{\kappa}_p + 2\kappa_d) \approx 3q^4 (D_2)^2 \approx \frac{3}{4}(\rho_{20})^2 \ . \tag{42}$$

As a final remark in this section, we point out that the coefficient of polarization transfer from ^{3}He to the neutron, κ_n, is equal to 1 in the spectator model. This follows immediately from Eq. (15).

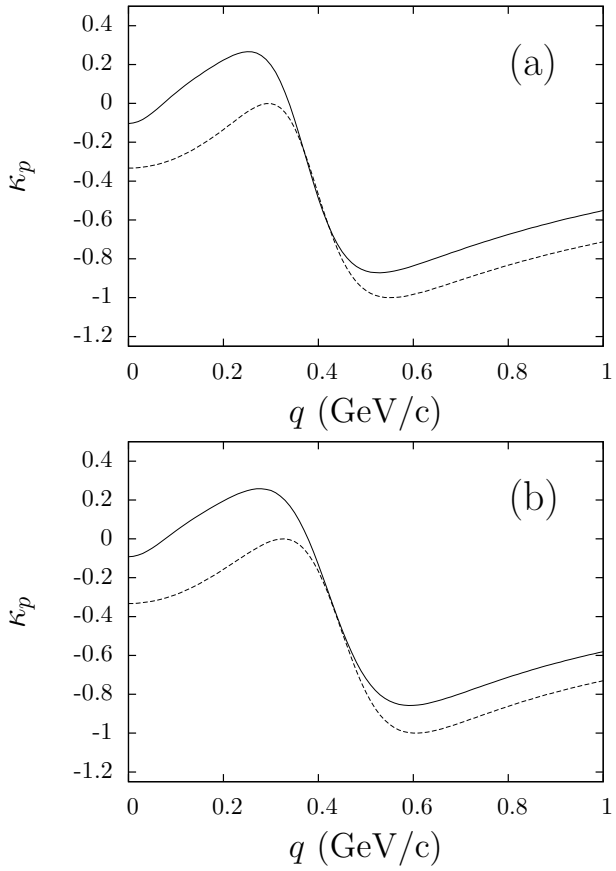

FIG. 7: The coefficient of polarization transfer from ^{3}He to the proton. The ^{3}He wave function used is based on the Paris potential (a) and the CD-Bonn potential (b). Solid line: Full wave function. Short-dashed line: only the $d + p$ projection (i.e., the $\widetilde{\kappa}_p$).

V. COMPARISON WITH EXPERIMENT

A. "Minimal relativization scheme"

To compare the calculated momentum distributions with experiment, it is necessary to establish a connection between the argument $\mathbf{q}$ of the ^{3}He wave function and the measured spectator momentum. This must be done in a way that allows one to take into account relativistic effects in ^{3}He.

This connection can be made in the framework of the so-called "minimal relativization scheme." In this approach, the relative momentum $\mathbf{q}$ between the pair and the spectator nucleon, taken in the ^{3}He rest frame, is replaced by the relativistic internal momentum $\mathbf{k} =$

$(\mathbf{k}_\perp, k_l)$, which appears in the light-cone dynamics. This is also referred to as the dynamics in the infinite momentum frame (IMF). The IMF is the limiting reference frame which is moving, with respect to the laboratory frame, in the negative z direction with a velocity that is close to the speed of light. The important question is how the light-cone variable $\mathbf{k}$ is connected with the measured momentum of the ^{3}He fragment.

In the IMF the nucleon momenta are parametrized as

$$
\begin{aligned}
p_1 &= \left((1-\alpha)\mathcal{P} + \frac{m^2+\mathbf{q}_\perp^2}{4(1-\alpha)\mathcal{P}}\,,\ \ \mathbf{q}_\perp,\right.\\
&\qquad\qquad \left.(1-\alpha)\mathcal{P} - \frac{m^2+\mathbf{q}_\perp^2}{4(1-\alpha)\mathcal{P}}\right),\\
p_2 &= \left(\beta\mathcal{P} + \frac{m^2+\left(\mathbf{p}_\perp - \frac{1}{2}\mathbf{q}_\perp\right)^2}{4\beta\mathcal{P}}\,,\ \ \mathbf{p}_\perp - \tfrac{1}{2}\mathbf{q}_\perp,\right.\\
&\qquad\qquad \left.\beta\mathcal{P} - \frac{m^2+\left(\mathbf{p}_\perp - \frac{1}{2}\mathbf{q}_\perp\right)^2}{4\beta\mathcal{P}}\right),\\
p_3 &= \left((\alpha-\beta)\mathcal{P} + \frac{m^2+\left(\mathbf{p}_\perp + \frac{1}{2}\mathbf{q}_\perp\right)^2}{4(\alpha-\beta)\mathcal{P}}\,,\ -\mathbf{p}_\perp - \tfrac{1}{2}\mathbf{q}_\perp,\right.\\
&\qquad\qquad \left.(\alpha-\beta)\mathcal{P} - \frac{m^2+\left(\mathbf{p}_\perp + \frac{1}{2}\mathbf{q}_\perp\right)^2}{4(\alpha-\beta)\mathcal{P}}\right)
\end{aligned}
\tag{43}
$$

with $0 \le \alpha \le 1$ and $0 \le \beta \le \alpha$. Here $\mathcal{P} \gg 3m$ is the IMF momentum of ^{3}He. The square of the $3N$ effective mass is

$$
\begin{aligned}
(\mathcal{M}_{3\mathrm{N}})^2 &= (p_1+p_2+p_3)^2\\
&= \frac{\alpha m^2 + (1-\alpha)(\mathcal{M}_{2\mathrm{N}})^2 + \mathbf{q}_\perp^2}{\alpha(1-\alpha)}\,,
\end{aligned}
\tag{44}
$$

where $(\mathcal{M}_{2\mathrm{N}})^2$ is effective mass squared of the pair:

$$
(\mathcal{M}_{2\mathrm{N}})^2 = (p_2+p_3)^2 = \frac{m^2 + \left[\mathbf{p}_\perp + \left(\frac{\beta}{\alpha} - \frac{1}{2}\right)\mathbf{q}_\perp\right]^2}{\frac{\beta}{\alpha}\left(1-\frac{\beta}{\alpha}\right)}\,.
\tag{45}
$$

The relative momentum between the relativistic spectator nucleon and the pair becomes

$$
k = |\mathbf{k}| = \sqrt{\frac{\lambda(\mathcal{M}_{3\mathrm{N}}^2, \mathcal{M}_{2\mathrm{N}}^2, m^2)}{4\mathcal{M}_{3\mathrm{N}}^2}}\,,
\tag{46}
$$

where $\lambda(a,b,c) = a^2+b^2+c^2-2ab-2ac-2bc$.

It should be noted that if the relative momentum in the pair is non-relativistic

$$
\frac{\beta}{\alpha} \approx \frac{1}{2},
\tag{47}
$$

then the effective mass $\mathcal{M}_{2\mathrm{N}}^2 \approx 4m^2$. In this case the problem is reduced to the relative motion of two particles with fixed masses, m and $M = 2m$, having spins $\frac{1}{2}$ and j, respectively.

We have calculated the average relative momentum squared $\langle p^2\rangle$ in different partial waves and have found that $\langle p^2\rangle < 0.08$ (GeV/c)^2 for the Paris potential and $\langle p^2\rangle \lesssim 0.1$ (GeV/c)^2 for the CD-Bonn potential when $q \lesssim 0.6$ GeV/c. This justifies the non-relativistic description of the relative motion in the pair and we therefore put $(\mathcal{M}_{2\mathrm{N}})^2 \approx 4m^2$.

The IMF variables α and $\mathbf{q}_\perp$ must now be connected with the appropriate kinematical variables measured in the $(^3\mathrm{He}, p)$ and $(^3\mathrm{He}, d)$ breakup experiments. In the laboratory frame we choose the z-axis along the ^{3}He momentum $P_\tau = (E_\tau, \mathbf{0}_\perp, P)$.

In the case of the $(^3\mathrm{He}, p)$ breakup the IMF variables α and $\mathbf{k}_\perp$ are defined by

$$
1-\alpha = \frac{E_p + p_l}{E_\tau + P}, \quad \mathbf{k}_\perp = \mathbf{q}_\perp\,,
\tag{48}
$$

where $p = (E_p, \mathbf{q}_\perp, p_l)$ is the proton four-momentum (its components are given here in the laboratory frame). For the $(^3\mathrm{He}, d)$ reaction the IMF variables are defined by

$$
\alpha = \frac{E_d + d_l}{E_\tau + P}, \quad \mathbf{k}_\perp = -\mathbf{q}_\perp\,,
\tag{49}
$$

where $d = (E_d, -\mathbf{q}_\perp, d_l)$ is the deuteron four-momentum.

In both cases the relativistic internal momentum in ^{3}He is

$$
\begin{aligned}
&\mathbf{k} = (\mathbf{k}_\perp, k_l)\ ;\\
&k_l = \pm\sqrt{\frac{\lambda(\mathcal{M}_{3\mathrm{N}}^2, M^2, m^2)}{4\mathcal{M}_{3\mathrm{N}}^2} - \mathbf{k}_\perp^2}, \qquad \mathbf{k}_\perp = \pm\mathbf{q}_\perp.
\end{aligned}
\tag{50}
$$

The signs "$-$" and "$+$" are chosen for $\alpha < \alpha_0$ and $\alpha > \alpha_0$ respectively; if $\alpha = \alpha_0$ then $k_l = 0$. Here $\alpha_0 = \sqrt{4m^2+\mathbf{q}_\perp^2}/\left(\sqrt{m^2+\mathbf{q}_\perp^2} + \sqrt{4m^2+\mathbf{q}_\perp^2}\right)$.

In the framework of the IMF dynamics the effective deuteron number is given by

$$
\begin{aligned}
\mathcal{N}_d^{\mathrm{ef}} &= \int d^3k d(k)\\
&= \int_0^1 d\alpha \int d^2k_\perp \frac{\varepsilon_p(k)\varepsilon_d(k)}{\alpha(1-\alpha)\mathcal{M}_{3\mathrm{N}}}\, d(k),
\end{aligned}
\tag{51}
$$

where $\varepsilon_p(k) = \sqrt{m^2+k^2}$, $\varepsilon_d(k) = \sqrt{M^2+k^2}$. The combination

$$
d^{\mathrm{rel}}(\alpha, \vec{k}_\perp) = \frac{\varepsilon_p(k)\varepsilon_d(k)}{\alpha(1-\alpha)\mathcal{M}_{3\mathrm{N}}} d(k)
\tag{52}
$$

can be considered as the relativized momentum distribution of the deuteron in ^{3}He.

The invariant differential cross section for the $A(^3\mathrm{He}, d)$ breakup is given by

$$
E_d \frac{d^3\sigma}{d\mathbf{p}_d} = f_{\mathrm{kin}}^{(d)} \sigma_p d^{\mathrm{rel}}(\alpha, \vec{k}_\perp),
\tag{53}
$$

where

$$
f_{\mathrm{kin}}^{(d)} = \frac{\lambda^{\frac{1}{2}}(W, m^2, M_A^2)}{(1-\alpha)M_A P},
\tag{54}
$$

W is the missing mass squared and M_A is the mass of the target nucleus.

Similarly, one can get the cross section for the $A(^3\mathrm{He}, p)$ breakup by

$$E_p \frac{d^3\sigma}{d\mathbf{p}_p} = f_{\rm kin}^{(p)} \sigma_d (1-\alpha) p^{\rm rel}(\alpha, \vec{k}_\perp), \qquad (55)$$

where

$$f_{\rm kin}^{(p)} = \frac{\lambda^{\frac{1}{2}}(W, M^2, M_A^2)}{2\alpha M_A P} \qquad (56)$$

and

$$p^{\rm rel}(\alpha, \vec{k}_\perp) = \frac{\varepsilon_p(k)\varepsilon_d(k)}{\alpha(1-\alpha)\mathcal{M}_{3\rm N}} p(k) \qquad (57)$$

is the relativized momentum distribution of the protons. The σ_p and σ_d factors appearing in Eqs. (53) and (55) play the roles here of normalization factors. Their physical interpretation is beyond the scope of the present paper.

B. Empirical momentum distributions

Equations (53) and (55) connect differential cross sections of the ^{3}He breakup reactions with the relativized momentum distributions. Dispite the fact that these equations were derived in the framework of the impulse approximation, one may expect that momentum distributions extracted from ^{12}C(^{3}He,p) and ^{12}C(^{3}He,d) breakup data, using Eqs. (53) and (55), include effectively effects beyond the impulse approximation, in particular, coming from quark structure of ^{3}He. We therefore call the extracted momentum distributions "empirical momentum distributions" (EMDs) of the spectators in ^{3}He.

In Fig. 8 we show EMDs for protons and deuterons in ^{3}He extracted from ^{12}C(^{3}He,p) and ^{12}C(^{3}He,d) breakup data obtained for fragments emitted at zero angle and at $p_{\rm He} = 10.8$ GeV/c [5]. These EMDs are compared with the results of our calculations using the Paris and CD-Bonn potentials. The empirical momentum distribution for the deuteron is also compared with results of other experiments. Good agreement between data and calculations is obvious at small $k \lesssim 0.25$ GeV/c, which indicates that in this region the spectator model can be used to interpret the data. Note that the difference between the light cone variable k and the spectator momentum taken in the ^{3}He rest frame is small in this region.

At very small $k \lesssim 50$ MeV/c there is an enhancement of the extracted EMDs over theoretical curves. A natural explanation of this enhancement appears to be a manifistation of Coulomb effects in ^{12}C(^{3}He,p) and ^{12}C(^{3}He,d) with registration of the spectator particle at zero angle. [3] We neglect such Coulomb effects because they take place only over a very narrow k region and do not affect the data interpretation elsewhere. Similarly, we neglect any possible final state interaction between the outgoing protons and deuterons.

It was shown in Ref. [5] that at higher spectator momenta the EMDs of deuterons and protons in ^{3}He plotted versus the relativized internal momentum k coincide well [which is consistent with the presentations in Fig. 2(b) and Fig. 4], while they are significantly different when plotted versus the non relativistic internal momentum (the spectator momentum in the ^{3}He rest frame). Such agreement only holds when the analysis is done in terms of the relativized internal momentum k. This indicates that the k variable is an adequate measure for the internal relative momentum of the ^{3}He constituents.

Data on (d, p) fragmentation [24], including those for spin-dependent observables [25, 26] and their analysis, resulted in similar conclusions. At small $k \lesssim 0.25$ GeV/c the spectator model can be used for the data analysis, the EMD of protons in the deuteron agrees well with the proton momentum distribution density calculated for known versions of the deuteron wave function, while at higher k there is a strong qualitative disagreement between calculations and the existing set of data. We therefore expect that in the ^{3}He breakup for $k \lesssim 250$ MeV/c the reliability of the spectator model predictions should be about the same as in the (d, p) case.

The data points for momenta above $k \sim 0.25$ GeV/c, where the distances between the ^{3}He constituents become comparable to the nucleon radius or even less, systematically exceed the calculated momentum distributions for both deuterons and protons. This is once again very similar to the excess of data over calculations in (d, p) fragmentation [24]. It was interpreted as a manifestation of the Pauli principle at the level of constituent quarks in the two-nucleon system [28]. It is possible that the observed enhancements in $(^3\mathrm{He}, d)$ and $(^3\mathrm{He}, p)$ reactions have the same nature. In other words, an extrapolation to this region of the wave function based on phenomenological realistic NN potentials for point-like nucleons is hard to justify.

C. Tensor polarization of the deuteron

Data on the tensor polarization ρ_{20} of the deuteron in the reaction ^{12}C(^{3}He, d) at several GeV have been published [10, 11]. It should, however, be noted that the preliminary data [11] extracted from this experiment have the opposite sign to those tabulated in the final data set [10].

On the other hand, the experimental value of the D_2

[3] See, e.g., Ref. [27], where a similar enhancement in the EMD of protons in the deuteron was explained as an effect of the Coulomb interaction on the mechanism of ^{12}C(d, p) breakup.

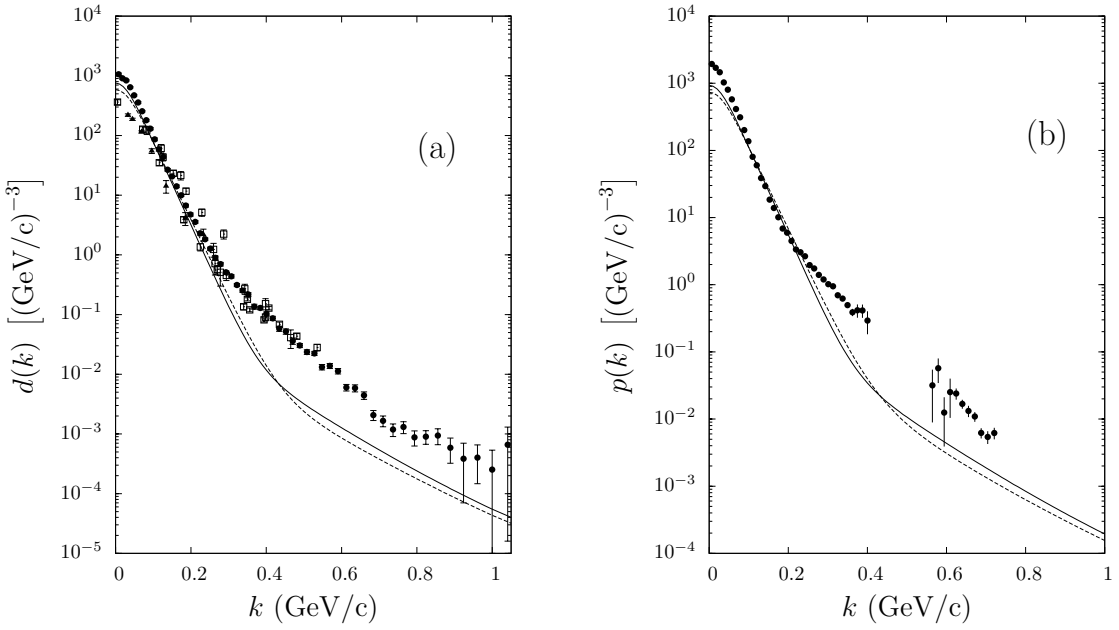

FIG. 8: The empirical momentum distribution of the deuterons (a) and the protons (b) in ^{3}He. The solid and dashed lines are calculated with the Paris and CD-Bonn potentials, respectively. Circles are for the empirical momentum distributions extracted within Eq. (53) (for deuterons) and Eq. (55) (for protons) from Ref. [5]. Squares and triangles represent data extracted from Refs. [6] and [7], respectively. The empirical proton momentum distribution is normalized to the calculated one for $k < 100$ MeV/c.

parameter for ^{3}He projected onto the $d+p$ channel has the opposite sign with respect to the experimental data on the similar D_2 parameter for the deuteron in the $n+p$ channel. Therefore the sign of the ρ_{20} under discussion must be opposite to that of the tensor analyzing power in the $d \to p$ breakup. Taking this into account, together with the contradiction in signs of ρ_{20} between Refs. [11] and [10], it is tempting to conclude that the data tabulated in Ref. [10] have the wrong sign. We therefore use the data from Ref. [10] but with a reversed sign and compare them in Fig. 9 with ρ_{20} calculated according Eq. (28).

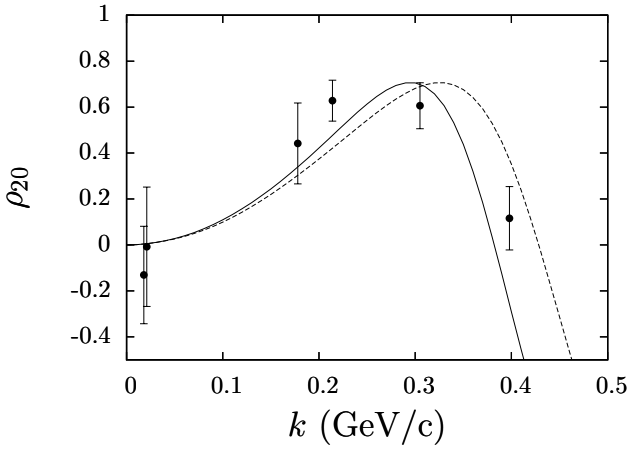

FIG. 9: Deuteron alignment ρ_{20} calculated with the ^{3}He wave functions for the Paris (solid) and CD-Bonn (dashed) potentials compared with experimental data. The signs of the data points [10] are reversed to bring them into accordance with the preliminary results [11] of the same experiment, as well as with the sign of experimental data on the D_2 parameter for ^{3}He.

Our results for other spin-dependent observables in the ^{3}He breakup cannot currently be compared with experiment because the relevant data base for spin-dependent observables is very scarce: at the present time there are no polarized ^{3}He beams with energies of several GeV/nucleon.

VI. CONCLUSIONS

Using a recent parametrization [14] of the fully antisymmetric three-nucleon wave function, based on the Paris and CD-Bonn potentials, we have presented here an analysis of the spin-dependent observables for $(^3\mathrm{He}, d)$ and $(^3\mathrm{He}, p)$ reactions, paying special attention to their behavior at small internal momenta of the ^{3}He fragments. This dependence is determined by a single parameter, known in the literature as the D_2 parameter. Some direct relations between experimental observables at small internal momenta of the ^{3}He fragments were obtained from this fact.

These relations are useful for the data base cross-checks; at low internal momenta of the fragments of ^{3}He, where the model used for the breakup reactions works

reasonably well, they are rather strict. The D_2 parameter completely determines both the sign and the q dependence of the observables at small ($\lesssim 150$ MeV/c) internal momenta.

On the other hand, these relations show that the breakup reactions with the lightest nuclei at intermediate energies provide a new way of obtaining experimental data on the D_2 parameter for these nuclei. This is complementary to the usual methods that involve rearrangement reactions at low energies.

We emphasize that the different conventions regarding the angular momentum summations for the $3N$ system result in different forms for the formulasconnecting spin-dependent observables with the ^{3}He wave function components. Of course, the final numerical results do not depend on the conventions provided that the calculations are performed systematically within one chosen scheme. However the occasional mixing of the schemes leads unavoidably to erroneous results. Therefore an explicit indication of the chosen angular momentum summation scheme is important for the applications. [4]

Comparing the results of calculations of the deuteron and proton momentum distributions in the ^{3}He nucleus with existing experimental data, we conclude that the model used for the ^{3}He breakup reactions works reasonably well for $k \lesssim 250$ MeV/c but at higher momenta the data and calculations are in systematic disagreement. This disagreement, i.e., the enhancement of the experimental momentum distributions over the calculated ones above $k \sim 0.25$ GeV/c is very similar to the enhancement of data over calculations observed for the (d,p) fragmentation [24] at small emission angles. This was interpreted for the two-nucleon system as a manifestation of the Pauli principle at the level of constituent quarks [28]. In other words, an extrapolation to this region of the wave function based on phenomenological realistic NN potentials for point like nucleons is questionable even when relativistic effects are taken into account within the framework of light cone dynamics.

[4] Perhaps the lack of such indication explains why the sign of the D wave, parametrized in Ref. [29] on the basis of values tabulated in Ref. [18], is opposite to that of the original tables.

Acknowledgments

The authors gratefully acknowledge Yuri Uzikov for fruitful discussions on various points considered in the present paper. We are indebted to Colin Wilkin for his invaluable help with the presentation of the work, as well as for useful discussions of the model considered. The work of A.P.K. was supported by the Research Programm "Research in Strong Interacting Matter and Hadron Dynamics in Relativistic Collisions of Hadrons and Nuclei" of the National Academy of Sciences of Ukraine.

Appendix A: The proton polarization in the (^{3}He, p) breakup reaction

The momentum distribution of a proton in ^{3}He is given by

$$p_{\sigma\xi}(q,\theta) = 3\int d^3p \left[\left| \chi_\xi^\dagger \langle 0010| \Psi_\sigma(\mathbf{p},\mathbf{q}) \right|^2 + \sum_{s_3} \left| \chi_\xi^\dagger \langle 1s_300| \Psi_\sigma(\mathbf{p},\mathbf{q}) \right|^2 \right], \tag{A1}$$

where σ and ξ are magnetic quantum numbers for ^{3}He and the proton, respectively, and θ is the angle between the quantization axis and the proton momentum $\mathbf{q}$. Let us consider the angular integration of the first and second terms in the square brackets of Eq. (A1):

$$\begin{aligned}
&\int d\Omega_p \left| \chi_\xi^\dagger \langle 0010| \Psi_\sigma(\mathbf{p},\mathbf{q}) \right|^2 = \frac{1}{4\pi}\frac{1}{3}\delta_{\xi,\sigma}\psi_1^2(p,q), \\
&\sum_{s_3}\int d\Omega_p \left| \chi_\xi^\dagger \langle 1s_300| \Psi_\sigma(\mathbf{p},\mathbf{q}) \right|^2 \\
&= 4\pi \sum_{s_3} \left| \frac{1}{4\pi} \left\langle 1\tfrac{1}{2} s_3 \xi | \tfrac{1}{2}\sigma \right\rangle \psi_2(p,q) - \sqrt{\frac{1}{4\pi}} \left\langle 1\tfrac{1}{2} s_3 \xi | \tfrac{3}{2} K_3 \right\rangle \left\langle \tfrac{3}{2} 2 K_3 L_3 | \tfrac{1}{2}\sigma \right\rangle Y_{1L_3}(\widehat{q}) \psi_3(p,q) \right|^2 \\
&+ \sum_{M} \left| -\sqrt{\frac{1}{4\pi}} \left\langle 1\tfrac{1}{2} M \xi | \tfrac{1}{2}\sigma \right\rangle \psi_4(p,q) + \left\langle 1\tfrac{1}{2} M \xi | \tfrac{3}{2} K_3 \right\rangle \left\langle \tfrac{3}{2} 2 K_3 L_3 | \tfrac{1}{2}\sigma \right\rangle Y_{1L_3}(\widehat{q}) \psi_5(p,q) \right|^2 \\
&= \frac{1}{4\pi} \sum_{i=2,4} \sum_{\rho} \left| \left\langle 1\tfrac{1}{2} \rho \xi | \tfrac{1}{2}\sigma \right\rangle \psi_i(p,q) - \sqrt{4\pi} \left\langle 1\tfrac{1}{2} s \rho \xi | \tfrac{3}{2} K_3 \right\rangle \left\langle \tfrac{3}{2} 2 K_3 L_3 | \tfrac{1}{2}\sigma \right\rangle Y_{1L_3}(\widehat{q}) \psi_{i+1}(p,q) \right|^2 .
\end{aligned} \tag{A2}$$

After straightforward calculations we arrive at

$$\begin{aligned}
\int d\Omega_p \left| \chi^\dagger_{\frac{1}{2}} \langle 1 s_3 00 | \, \Psi_{\frac{1}{2}}(\mathbf{p},\mathbf{q}) \right|^2 &= \frac{1}{4\pi} \left\{ \frac{1}{3} \left[\psi_2^2(p,q) + \psi_4^2(p,q) \right] + \frac{1}{2} \left(\frac{1}{3} + \cos^2\theta \right) \left[\psi_3^2(p,q) + \psi_5^2(p,q) \right] \right. \\
&\left. + \sqrt{2} \left(\frac{1}{3} - \cos^2\theta \right) \left[\psi_2(p,q)\psi_3(p,q) + \psi_4(p,q)\psi_5(p,q) \right] \right\}, \\
\int d\Omega_p \left| \chi^\dagger_{-\frac{1}{2}} \langle 1 s_3 00 | \, \Psi_{\frac{1}{2}}(\mathbf{p},\mathbf{q}) \right|^2 &= \frac{1}{4\pi} \left\{ \frac{2}{3} \left[\psi_2^2(p,q) + \psi_4^2(p,q) \right] + \frac{1}{2} \left(\frac{5}{3} - \cos^2\theta \right) \left[\psi_3^2(p,q) + \psi_5^2(p,q) \right] \right. \\
&\left. - \sqrt{2} \left(\frac{1}{3} - \cos^2\theta \right) \left[\psi_2(p,q)\psi_3(p,q) + \psi_4(p,q)\psi_5(p,q) \right] \right\} \, .
\end{aligned} \tag{A3}$$

[1] E. Jans et al., Phys. Rev. Lett. **49**, 974 (1982).
[2] M. M. Rvachev et al., Phys. Rev. Lett. **94**, 192302 (2005).
[3] C. Marchand et al., Phys. Rev. Lett. **60**, 1703 (1988).
[4] R. Florizone et al., Phys. Rev. Lett. **83**, 2308 (1999).
[5] V. G. Ableev et al., JETP Lett. **45**, 596 (1987) [Pis'ma v ZhETF **45**, 467 (1987)].
[6] P. Kitching et al., Phys. Rev. C **6**, 769 (1972).
[7] M. V. Epstein et al., Phys. Rev. C **32**, 967 (1985).
[8] C. C. Kim et al., Nucl. Phys. **58**, 32 (1964); L. G. Votta et al., Phys. Rev. C **10**, 520 (1974); H. Langevin-Joliot et al., Nucl. Phys. A **158**, 309 (1970); R. Frascaria et al., Phys. Lett. B **66**, 329 (1977); P. Berthet et al., Phys. Lett. B **106**, 465 (1981).
[9] Y. Shimizu et al., Phys. Rev. C **76**, 044003 (2007).
[10] I. M. Sitnik et al., Phys. Rev. C **84**, 034006 (2011).
[11] I. M. Sitnik et al., Nucl. Phys. A **663**, 443 (2000).
[12] M. Lacombe et al., Phys. Rev. C **21**, 861 (1980).
[13] R. Machleidt, Phys. Rev. C **63**, 024001 (2001).
[14] V. Baru, J. Haidenbauer, C. Hanhart, and J. A. Niskanen, Eur. Phys. J. A **16**, 437 (2003).
[15] W. Schadow, W. Sandhas, J. Haidenbauer, and A. Nogga, Few Body Systems **28**, 241 (2000).
[16] L. D. Knutson et al., Phys. Rev. Lett. **35**, 1570 (1975).
[17] J. L. Friar, B. F. Gibson, D. R. Lehman, G. L. Payne, Phys. Rev. C **25**, 1616 (1982) and references therein.
[18] R. Schiavilla, V. R. Pandaripande and R. B. Wiringa, Nucl. Phys. A **449**, 219 (1986).
[19] A. P. Kobushkin, Deuteron-93, Proc. Int. Symposium "Dubna Deuteron-93", Dubna, Sept. 14-18, 1993, JINR, E2-94-95 (1994), p.71.
[20] M. E. Brandan and W. Haeberli, Nucl. Phys. A **287**, 213 (1977).
[21] S. Roman et al., Nucl. Phys. A **289**, 269 (1977).
[22] S. Sen and L. D. Knutson, Phys. Rev. C **26**, 257 (1982).
[23] I. M. Sitnik et al., JINR preprint E1-94-186 (1994); Proc. Int. Symposium "Dubna Deuteron-93", Dubna, Sept. 14-18, 1993, JINR, E2-94-95 (1994), p.282.
[24] V. G. Ableev et al., Nucl. Phys. A **393**, 491 (1983) and Nucl. Phys. A **411** 541 (E) (1983); V. G. Ableev et al., JINR Rapid Comm. **1[52]-92**, 10 (1992); V. G. Ableev et al., JINR Rapid Comm. **1[52]-92**, 5 (1992) and Yadernaya Fizika **37**, 132 (1983) (in Russian).
[25] See, for example, C. F. Perdrisat et al., Phys. Rev. Lett. **59**, 2840 (1987); V. Punjabi et al., Phys. Rev. C **39**, 608 (1989); L. S. Azhgirey et al., Phys. Lett. B **387**, 37 (1996).
[26] V. G. Ableev et al., JINR Rapid Comm. **4[43]-90**, 5 (1990); first data in Pis'ma v ZhETF **47** 558 (1988); B. Kuehn et al., Phys. Lett. B **334**, 298 (1994); L. S. Azhgirey et al., JINR Rapid Comm. **3[77]-96**, 23 (1996).
[27] A. P. Kobushkin, Ya. D. Krivenko-Emetov, Ukr. J. Phys. **53**, 751 (2008).
[28] A. P. Kobushkin, Phys. Lett. B **421**, 53 (1998); Phys. Atom. Nucl. **62**, 1140 (1999) 1140 [Yad. Fiz. **62**, 1213 (1999)].
[29] J. - F. Germond and C. Wilkin, J. Phys. G: Nucl. Phys. **14**, 181 (1988).